Available online at www.sciencedirect.com

ScienceDirect

Energy Procedia 81 (2015) 1184 – 1197

Energy Procedia

69th Conference of the Italian Thermal Engineering Association, ATI 2014

Power Reduction in Vapour Compression Cooling Cycles by Power Regeneration

Ascani Maurizio[a], Cerri Giovanni[b]*, De Francesco Eduardo[c]

[a]*Angelantoni Industrie S.p.A., loc. Cimacolle, 464, 06056 Massa Martana (PG), Italy*

[b]*Roma Tre University, Department of Engineering, Via della Vasca Navale, 79, 00146 Rome, Italy*

[c]*Se.Te.L S. r. l., Via Casamari, 6, 00142 Rome, Italy*

Abstract

Many attempts have been made to save the power consumed by the Main Compressors of Refrigeration Plants. This paper deals with the adoption of a special technique based on the power regeneration by internal cycles to reduce the Vapour Compression Refrigeration Plant Power. In the paper, the possibility to optimize a cooling plant layout leading to an expected power decrement of some 23 - 26% is demonstrated. Car Engine Turbocharger Technology has been adopted to produce an innovative Compressor Expander Group (CEG).

Experiments on an *ad hoc* built Test Bench have shown the positive response of the system and the possibility of development of an innovative technology regarding the CEG.

Peer-review under responsibility of the Scientific Committee of ATI 2014

Keywords: Refrigeration Plant; Vapour Pressure Amplifier; Vapour Pressure Booster; Compressor Expander Group; Power Saving; Centrifugal Compressor; Radial Inflow Turbine; Condensate Subcooling; Cryogenic Plants.

1. Introduction

Artificial COOL is a good widely used by human beings for refrigeration and air conditioning purposes. Vapour Compression Refrigeration Systems (VCRS) are the most used and are driven mainly by electric power. Domestic refrigeration, food processing and cold storage, refrigeration of industrial processes, transport refrigeration,

* Corresponding author. Tel.: +39-0-657-333-251; fax.: +39-0-657-333-650.
E-mail address: cerri@uniroma3.it

Peer-review under responsibility of the Scientific Committee of ATI 2014
doi:10.1016/j.egypro.2015.12.148

electronic device cooling, air conditioning, are the major relevant VCRS applications among the vast number of cases. Unit Cool Power (CP) may range from few hundred watts to more than 10 MW. The worldwide-consumed electric energy by VCRSs is an enormous quantity being some 15% of the whole one. Some 4.5% of the greenhouse effect total gas emissions is connected with such an electricity production. The millions of litres of gasoline, diesel fuel, liquid & Natural Gas burned to power cars trucks and ships air conditioners and refrigerators, must be added to the above consumption [1, 2]. It can be easily understood that a small percentage of power saving per unit of produced cool leads to an enormous amount of primary energy saving and of CO2 and other pollutant emissions. For these reasons, there is a continuous search to improve the VCRS Coefficient of Performance (COP) through the definition of new refrigerants and implementation of innovations in the cycle arrangements introducing new devices.

Conventional VCRS power saving methods are based on the increase of condensate subcooling, the adoption of ejector loops, the addition of flash tanks for multistage cycles, also trials to substitute the throttling valve with expanders used to reduce the main compressor power. An amply literature survey on VCRS cycle modifications is given in [3]. Also in [4] a literature review on two-phase ejector applications to VCRS is presented and discussed with COP improvements being analysed. Other main compressor power saving for constant cool power and cycle modifications for performance improvements have been reported in recent papers [5-12]. In addition, the adoption of Liquid Pressure Amplifiers has been analysed and experimented [13-15]. Various patents have been applied in this context [16-21]. Fig. 1 shows the scheme and the cycle of the [21] patent that appears as the most attractive in terms of feasibility and expected VCRS main compressor power saving for fixed cool power. COLD ENERGY research project subject has been the development of the crucial components for the patent concept demonstration. The Fig. 1 cycle has been named Power Recovered Cycle (PRC) and the paper presents the concepts that lead to improved COP owing to the lower Main Compressor Power taken from the outside for constant CP.

The cycle optimization taking the machine features into consideration as well as the limiting quantities of the Bleed Evaporators will be discussed with reference to a special cryogenic refrigeration plant that has been taken as reference for the experimental activity. The characteristics of the expander and compressor will be discussed together with the design philosophy. The designed machines and their tests carried on the Refrigeration Test Bench will be presented and results commented.

Nomenclature

β	Pressure Ratio
Cs	Sound Speed
C_{SP}	Spouting Velocity
Δ	Difference
D	Data, Diameter
ξ	Degree of Freedom
Ds	Specific Diameter
η	Efficiency
G	Dependent Variables
γ	Relative Velocity Flow Angle, Blade Angle
g_c	Geometric Variables of the Components
g_m	Geometric Shape
H, h	Enthalpy
m	Mass Flow Rate
Ma	Mach Number
μ	Dynamic Viscosity
n	Rotational Speed (rpm)
ν	Kinematic Viscosity
ω_s	Specific Speed
ω_{sc}	Specific Speed of Compressor
P	Power
p	Pressure
π	Pi Number
Qc	Cool Power
Re	Reynolds Number
ρ	Density
T	Temperature
U	Peripheral Velocity
V	Volumetric Flow
WF	Working Fluid
Z_b	Number of Bleeds

Subscripts

A	approach
b	bleed, blade
bgv	bleed generator vapour
c	compressor, condenser
ce	cooling effect
e	expander, evaporator
g	group
i, j, k	order number
in	inlet
kin	kinematic
l	lower

Subscripts (continue)

m	mechanical
mc, MC	main compressor
pp	pinch point
rc	recovery compressor
s	isentropic, saturated
sc	simple cycle
sh	superheating

Acronyms

BEVs	Bleed Expansion Valves
BT	Best Technology
BVGs	Bleed Vapour Generators
CE	Cooling Effect
CEG	Compressor Expander Group
CETT Technology	Car Engine Turbocharger
CFD	Computational Fluid Dynamic
COP	Coefficient Of Performance
CP	Cool Power
DOF	Degree of Freedom

Acronyms (continue)

FM & ECSG	Fluid Machinery and Energy Conversion Systems Group
HPB	High Pressure Bleed
IPRCs Cycles	Internal Power Regeneration
LP	Low Pressure
MC	Main Compressor
MCP	Main Compressor Power
OF	Objective Function
PD	Pressure Difference
PRC	Power Recovered Cycle; Power Recovery Compressor
RC	Recovery Compressor
SC	Simple Cycle
VCRC	Vapour Compression Refrigeration Cycles
VCRS	Vapour Compression Refrigeration Systems
VPA	Vapour Pressure Amplifier
VR	Velocity Ratio

Fig 1. Scheme of the refrigeration plant showing the devices of the [18] patent and the related cycle

2. Scientific & Technical Background

Refrigeration cycles are systems by which heat is removed from an enclosed space by the action of a colder surface that is kept at a temperature lower than the surrounding by the action of a refrigerant that moves through the cycle components. Vapour Compression Refrigeration Cycles (VCRC) are taken into consideration in this paper.

The low temperature (pressure) Main Evaporator (ME) provides the extraction of the heat power as CP. The high temperature (pressure) condenser rejects it into the environment (directly or by an intermediate fluid loop). A Main Compressor (MC) accomplishes the transfer of the refrigerant from the low evaporator pressure to the high condenser pressure absorbing Power from the outside. A Main Expansion Valve (MEV), usually, closes the cycle. Fig. 1 shows the Simple Cycle (SC) points: 1sc, 2sc, 5, 8sc, 1sc.

Many attempts have been done to reduce the power inputted into the compressor for a given CP. Among the various tries, the one based on the Power Recovery by means of Internal Power Regeneration Cycles (IPRCs) is investigated. IPRCs are performed by streams extracted from the condensate refrigerant. Suitable Bleed Expansion Valves (BEVs) reduce the direct cycle bleed stream pressures and temperatures. Then the bleed streams evaporate and superheat receiving the heat from the high-pressure condensate. The Cooling Effect (CE) rises owing to the additional condensate Subcooling and consequently, for a given CP, the mass flow rate through the ME decreases. Each bleed superheated refrigerant stream is processed by an Expander that drives a Power Recovery Compressor (PRC) increasing the pressure of the refrigerant from the ME. The bleed streams and the refrigerant from the PRC feed directly the MC. If the Degree of Freedom quantities are suitably chosen, the MCP is reduced. Thus the COP (i.e. the ratio between the CP and the MCP) rises.

Generic Power Recovered Cycle

Fig. 1 shows the generic scheme of an internally power regenerated refrigeration plant equipped with two bleeds, two BEVs, two Bleed Vapour Generators (BVGs), and two expanders driving a compressor by means of a single shaft. The bleed streams are fed into the MC inlet together with the compressed flow from the ME. Such a plant interact with the cold and hot surroundings and with the power source by the cycle points: 1, 2, 7, 8, and 10 as shown in the cycle depicted in the same figure.

Details of the IPRC models are given elsewhere [22] here global outlines are stated. Variables and equations refer to the cycle specification and to the selection and sizing of the Vapour Compressor Booster (VPB). The latter receives one or more High Pressure Bleeds (HPB) forceful flows and a Low Pressure flow from the Evaporator (LPE) and delivers both the entering mass flows at an Intermediate Pressure towards the MC inlet section. Various solutions are possible for the VPB; in the Cold Energy project, a turbomachine based solution has been explored because of the highest expected VPB efficiency, less weight, cost and lack of time for development.

The IPRC component specification refers to a generic plant like that shown in Fig. 1 and processes like the bleed evaporation and superheating that occurs in the BVG. Variables can be classified as data **D,** Degree of Freedom $\boldsymbol{\xi}$ and dependent ones **G** arrays:

- $G = \left| MCP,\ \Delta h_{ce}, m_{MC}, m_{bj}\ , m_e, m_{cj}, \Delta h_{MC}, \Delta h_{bgvj}, \Delta h_{ej}, \Delta h_{cj}, p_k, T_k, p_k, v_k, h_k, COP, \eta_{ej}, \eta_{cj}, \eta_{mj}, n_j, \mathrm{g}_{ci} \right|$
- $D = |\mathrm{Q_c}, \mathrm{T_c}, \mathrm{T_e}, \Delta \mathrm{T_{sh}}, \Delta \mathrm{T_{sc}}, \mathrm{WF}|$
- $\xi = \left| \mathrm{b}, \mathrm{T_{sbj}}, \Delta \mathrm{T_{ppj}}, \Delta \mathrm{T_{Aj}}, \omega_{\mathrm{csj}} \right|$

  $\forall\ \mathrm{k} = 1 - \mathrm{CPN};\ \ \forall \mathrm{j} = 1 - \mathrm{b};\ \ \forall \mathrm{i} = 1 - \mathrm{CN}$

CPN being the number of the cycle points; b being the number of bleeds; CN being the component number.
Equations in the following set

$$\mathrm{G} = \mathrm{F}(D, \xi) \tag{1}$$

describe conservation of mass, energy, momentum and entropy, the Working Fluid properties, and auxiliary equations representing the empirical relationships concerning the component performance versus the related variables (i.e. component technology).They establish the calculation models to be solved by a simultaneous solution technique based on cycle and component sizing procedure as described in [22]. This solution method requires establishing a suitable Objective Function (OF) minimization process being constrained by the equation set (1) and by bound conditions expressed as inequalities. The optimized solution leads to establish also the $\mathbf{g}_{ci}$ sets of geometric variables of the components influencing the objective function. Parallel design processes led to establish the other component sizes.

Innovative aspect of this research activity is the selection of the Compressor and Expander units to arrange the Compressor Expander Groups (CEGs) by choosing and modifying items included in an available turbomachinery technology.

The MCP represents the OF to be minimized given the **D** set. Concerning the Degree Of Freedom (DOF) the following can be stated:

- ΔT_{ppj} and $\Delta T_{Aj,}$ being the pinch point and the approach temperature differences in the BVGs, lower they are lower the MCP is. Reducing such temperature differences, the sizes of the BVGs become larger and larger increasing also the initial costs of the plant. The right compromise consists in establishing the lower bounds for them (ΔT_{ppj}^{l} and ΔT_{Aj}^{l});
- b, being the number of bleeds; the higher b, the lower MCP. Increasing b, the MCP step reduction becomes lower and lower while the plant initial cost rises. Thus, b (1 to 3) can be assumed depending on the application;
- ΔT_{sbj} ∀ j=1-b, being the saturation temperatures of the bleed inside each jth BVGj can be optimized to achieve the best OF;
- $\omega_{csj,}$ being the specific angular speed of each j compressor to be selected, leads to the geometry selection of turbomachinery to achieve the best efficiency of the jth CEG ($\eta_g = \eta_{cj} \cdot \eta_{ej} \cdot \eta_{mj}$). Thus, ω_{csj} optimum values have to be searched.

According to the above, ΔT_{sbj} and ω_{csj} ∀j=1-b are the DOFs to be optimized.

Compressor Expander Group

Models for CEG turbomachine selection, sizing and efficiency evaluation are required for the solution of the optimization process. The outcome is used for the detailed design to build the CEG. The model is based on the concept that, for any feasible set of variables (including efficiencies of turbomachines), the CEG adiabatic expansion and compression processes can be described as function of the thermodynamic quantities of the initial points (turbomachine inlet), local pressure and loss coefficients. For each turbomachinery, the mass flow rates as well as the volumetric flow rates are known. It can be easily understood that the sizing process of the CEGs is based on an iterative procedure established on compressor and expander efficiencies to be exchanged with the cycle model and then contributing to the OF. Two activity levels concerning a given turbomachinery technology can be identified. The first one regards the selection of turbomachinery and the second one consists in the sizing of them for the CEG performance evaluation. Due to the lack of a wide empirical knowledge for this application and the practical absence of a commercially available items, it has been decided the adoption of Car Engine Turbocharger Technology (CETT). They are built in millions of units, they work under severe conditions and they show very good fluid flow performance. Then high availability, reliability and efficiencies are expected together with low cost for the CEG. Selection has been made taking similitude rules into consideration. Similarity concepts mean that turbomachines being geometrically similar (i.e. they have the same shape - equal angles), working under kinematic similarity (i.e. triangles of velocities are similar - same vertex angles) and operating with flow fields having the same Reynolds and Mach numbers, show the same efficiencies. V volumetric flow rate (at the inducer for compressors and at the exducer for expander); D wheel diameter (exducer for compressors and inducer for expander); ρ working fluid density; μ fluid dynamic viscosity; C_s working fluid speed of sound; Δh_s isentropic enthalpy difference across the machine; n rotational speed (rpm) variables have been taken into consideration.

A turbomachinery geometric shape (g_m) being connected to a flow field shape, leads to performance that can be described as function of four no-dimensional groups: ω_s specific angular speed; D_s specific diameter; Re Reynolds number and Ma Mach number. For sufficiently high Reynolds number (10^6) losses are almost insensitive to it. Mach number sufficiently lower than 1 also shows little influence. In CETT, exhaust expansion takes place at temperatures between 900 and 1200 K and higher while air compression starts around 300 K. R404a sound speed ranges from 140 to 165 m/s. To avoid efficiency penalties, the wheel Mach number of high efficiency air (exhaust) operated machines has to be kept lower in turbomachines working with R404a. Working fluid R404a sound speed is about 44% of the air when these fluids are compressed. This ratio becomes some 25% when engine exhaust gas and R404a expand. Mach number preservation and similar velocity triangles imply changes in peripheral velocities. Therefore, accordingly to the sound speed ratio in the expander, the rotational speed must vary. The ratio between the kinematic viscosity of the air (exhaust) and the one of the R404a is higher than this application. Therefore, for equal

size turbomachines, the R404a Reynolds number is not relevant. According to the above only ω_s and D_s are sufficient to describe performance of geometrically similar machines operating with different working fluids under kinematic similarity (similar triangles of velocity). According to Similitude [23-26], the concepts of specific speed and specific diameter have been taken into consideration to establish the empirical relationship

$$f_{Ds}(\omega_s, D_s, \eta, g_m) = 0 \tag{2}$$

that depends on the main flow field shape related to the turbomachine geometry.
For compressors, this equation leads to establish a relationship

$$f(n, D, \eta, Z_b, \gamma, \Delta H_s, \nu_{kin}, \omega_{cs}) = 0 \tag{3}$$

that, for given geometry shape and blade number under flow similarity (similar velocity triangles), leads to

$$f(\omega_s, \eta) = 0 \tag{4}$$

Any technology level characterized by congruent or similarly shaped compressors can be classified by a Database and their single wheels can be modified to be adapted to the new needs $(V_{in}, \Delta H_s, \rho_{in})$ with the efficiency that is achievable using such a technology.

For expanders, equation (2) is substituted by the product between ω_s and D_s leading to Velocity Ratio (VR) that is the ratio between the peripheral velocity and the spouting one. It can be expressed as function of n, D and ΔH_S:

$$VR = \frac{U}{C_{SP}} = \frac{\pi \cdot D \cdot n}{60 \cdot \sqrt{2 \cdot \Delta H_S}} \tag{5}$$

Its value has to range from 0.60 to 0.80 for expanders reaching high efficiencies. Moreover, for radially oriented rotor blade leading edges, the inlet angle of the relative velocity have to be kept between 25 and 50 degs in respect to the peripheral tangent of the wheel [25,26]. To privilege efficiency, partial admission expanders must be always avoided, and then stator nozzles have to distribute the flow all around the wheel periphery. The radial gap circle of the stator blades trailing edges and the rotor inducer diameter is related to the blade height by a coefficient depending on the flow Mach number and nozzle geometry. Suggestions contained in [24-32] are taken into consideration to design a high performance turbine.

Turbomachinery Selection from a Technology

The selection of the compressor and expander wheel geometries is a rather complex task. One approach is consists in selecting the Best Technology solution that means the achievement of the best efficiency of the CEG. In this case a long development is necessary to asses by accurate 3D CFD the geometries that are chosen by the similitude concepts.

Due to time and cost constraints, it has been decided to adopt the Car Engine Turbocharger Technology. The selection is related to the:

- Compressor- made by the wheel and unbladed diffuser;
- Expander- made by nozzle blades, the wheel and the exit diffuser;
- Shaft and bearing central housing to meet the torque needs.

CETT empirical Database need to be used. Fig. 2 shows a CETT Compressor map and the empirical Data Base. The top right figure shows for a specified pressure ratio, the efficiency, the rotational speed, the specific angular

speed, and the corrected mass flow rate versus the volumetric flow rate entering the compressor. Each point correspond to a wheel of a unit of the family associated to an O&M. The bottom left figure gives a single wheel performance taken along the maximum efficiency curve. Such data are the efficiency, the pressure ratio, the rotational speed, the specific angular speed, the specific diameter, the Best Technology specific diameter [25, 26] versus volumetric flow rate. In the bottom right figure, the same data are reported versus the specific angular speed together with the product between the specific diameter and the specific angular speed. In addition, the Best Technology data are given.

CETT expander wheels usually are rigidly connected (welded) with the shaft. Since there is a strong reduction in the rotational speed, the expander size is selected taking the torque that the shaft is able to withstand.

3. IPRC demonstration

The IPRC concept experimental demonstration has been performed by building a cryogenic cooling plant for 100 kW cool power, R404a being the working fluid for such a plant. The design main evaporator temperature T_e = -40°C (P_e=133kPa) and the condenser one T_c = + 40°C (P_c=1830kPa) have been selected. The scheme of Fig. 3 shows two bleeds for condensate subcooling purposes and only one CEG installed in the highest-pressure bleed stream, the lowest pressure bleed being discharged directly into the MC inlet, downstream of the Recovery Compressor (RC).

Cycle optimization results

The plant cycle has been optimized to achieve the minimum MCP consumption by using the above-described models, procedures and methodologies.

Quantities that have been assumed for the design are: working Fluid R404a; T_c=40 °C; T_e= -40 °C; ΔT_{sh}=5 °C; ΔT_{sc}=5°C; ΔT_{ppj}=30 °C; ΔT_{Aj}=30 °C; b=2; The Main Compressor efficiency has also been assumed according to the applications in the field. The well-established Simultaneous Solution Methodology used by Roma Tre Fluid Machinery and Energy Conversion Systems Group (FM & ECSG) [22] has been used to accomplish evaluations.

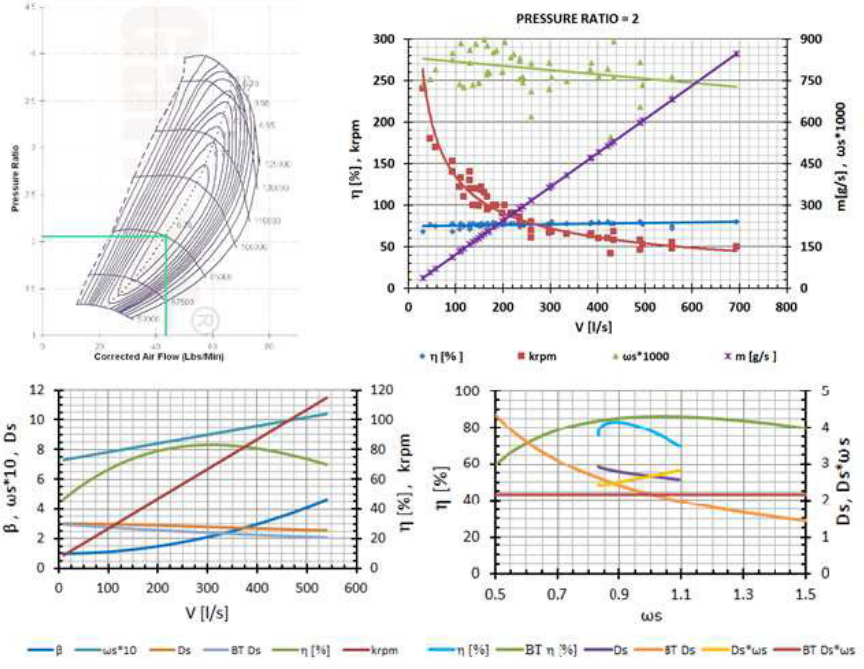

Fig. 2. CETT compressor database

Calculations have also been performed for four cases: Simple Cycle (as reference); one bleed (1B1CEG); two bleeds with two CEGs (2B2CEG); two bleeds with one CEG (2B1CEG), the second bleed being discharged after the heat transfer device directly into the Main Compressor inlet manifold. Comparative results are shown in table 1 where in the columns are given, cases that have been elaborated and in the rows there are the plant quantities.

It can be observed that in all the IPRC cases the MCP has strong reduction in respect to the SC. The adoption of two bleeds with one CEG installed on the highest Pressure bleed and the second bleed being used for condensate subcooling purposes and being injected downstream of the HPB Recovery Compressor, in the MC inlet section, has been chosen as demonstrator plant**.**

Table 1. Optimum calculations of IPRC options

A QUANTITY	B SC	C 1B1CEG	D (C-B)/B %	E 2B1CEG	F (E-B)/B %	G 2B2CEG	H (G-B)/B %
QC KW	100.00	100.00	0	100.00	0	100.00	0
PMC KW	101.50	78.53	-23	74.98	-26	74.31	-27
COP	0.98	1.27	30	1.33	36	1.35	38
ΔHCE KJ/KG	84.18	142.71	70	178.20	112	168.21	100
MMC KG/S	1.19	1.06	-11	1.05	-12	1.07	-10
MB1 KG/S		0.36		0.31		0.32	
MRC1 KG/S		0.70		0.56		0.54	
MB2 KG/S				0.18		0.15	
MRC2 KG/S						0.06	

Demonstrator Test Bench

The optimized 2B1CEG scheme is shown in Fig. 3 and has been calculated by the above methodology. The CEG data are given in Fig. 4. It can observed that vapour by-pass connects the MC exit to the Expander to have the possibility of modifying the CEG rotational speed. In Fig. 3, also the control system has been given.

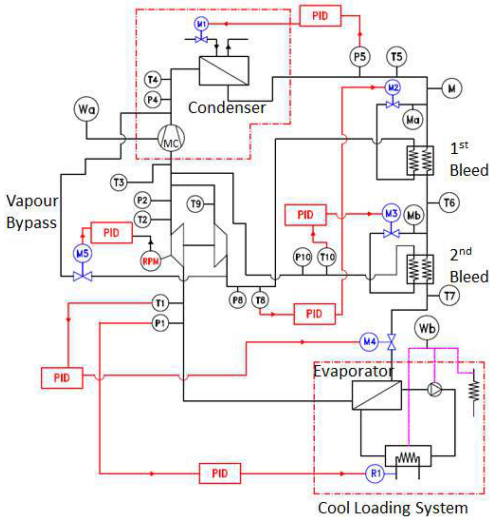

Fig. 3. Scheme of the demonstrator layout

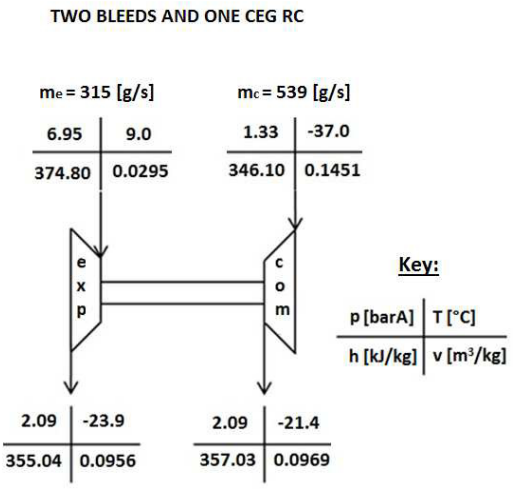

Fig. 4. CEG optimized thermodynamic and flow data

4. Test Bench and Experimental Set Up

According to the simulated results, a test bench based on the scheme of Fig. 3 has been designed, components have been manufactured and assembled together to set up the test bench. The various sections are briefly illustrated in the following.

Refrigeration loop

The plant is composed of various sections:

1. The cold loading system that is for the production of the heat power to be exchanged in the evaporator at a given temperature T_e. Heat Power can be set up to about 200kW and T_e from - 45°C to - 20°C. Both these two quantities can be kept constant in the time each independently from the other;
2. The condensing section allows keeping the temperature T_c constant in the time. T_c can be set in agreement with the experiment boundary conditions. Its lower value is related to the temperature of the water from the tower;
3. Two bleeds have been derived and equipped with the relative bleed expansion valves and bleed vapour generators;
4. The High Pressure Bleed has been equipped with a CEG container to avoid Refrigerant leaks and contamination. Photo of Fig. 5 gives an idea of the containment system.

Data acquisition system

This system allows acquiring all the analogical and digital nature signals. They are generated by the system. Based on the signals acquired and on the parameters, which can be defined by the system operator, the application allows the following functionalities:

- The management of the alarms;
- The control of motorized valves;
- The calculation of many thermodynamic parameters;
- The visualization on a synoptic representing the plant scheme of the alarms measured and calculated quantities;
- The recording of the useful data.

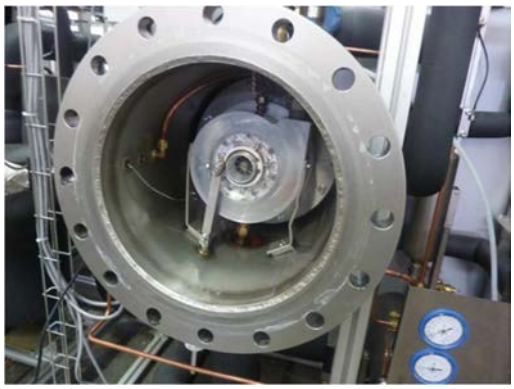

Fig. 5. CEG Installed in the Cold Energy Test Bench

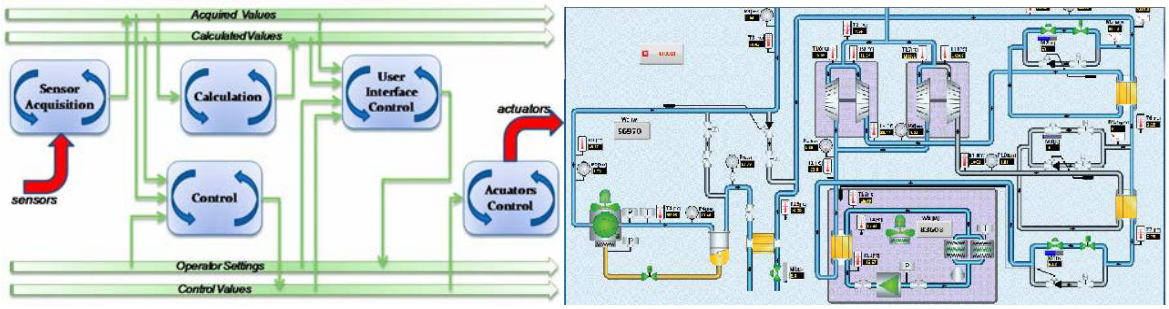

Fig. 6. Bloc scheme of the key operators and synoptic view of the test bench P. & I.

The software architecture allows each module to operate independently each other. This for a more accurate timing. The information transfer between modules is realized using global shared variables, which can be accessed by all modules at any time. In the previous Fig. 6, the key global variables are shown as databases where specific modules can, at any time, read and write data. The scheme shows the types of access which each module implement on the different databases. The synoptic drawing of the plant on a computer screen is shown in this figure.

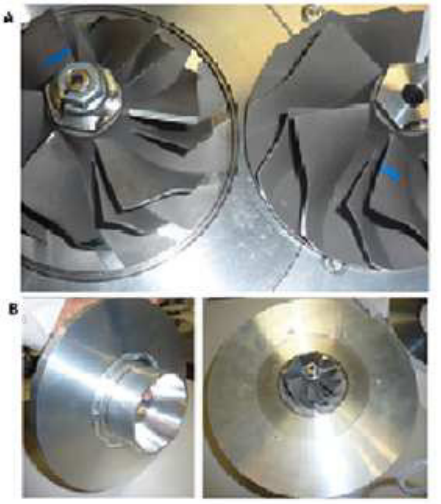

Fig. 7. Photos of compressor wheel (A), front & rear disks (B)

Compressor Expander Group

Decisions connected with the timing and the funding for the R&D activities have led to the use of the CETT to avoid some time consuming and costing investigations.
The various selections have been connected with the sizing of:

- Compressor wheel and diffuser
- Expander wheel, nozzle blading and exit diffuser
- Shaft and Bearing Housing

Moreover, the expander nozzle that guides the flow into the turbine wheel has been designed (see Fig. 8). In addition, the lubrication system has to be taken into consideration.

Compressor wheel selection

Since the inducer blade angle being unchanged and the refrigerant incidence angle as to be equal to that of the air best efficiency, the selection is made according to the specific speed (i.e. similar inlet velocity triangles and inlet flow shapes). Among the various candidates, the choice has been made taking into consideration the exducer diameter. It has been machined to accommodate both the total enthalpy rise and the exit volumetric flow to have similar triangles of velocity. Photos of Fig. 7 show the compressor wheel after modification; the left hand rotor blades have been cut. In addition, the casing rear and front disks with the inlet duct are given in the same figure.

Expander wheel and shaft assembly

Expander wheel is rigidly welded with the shaft. It has to be selected taking the torque to be transmitted into account, because the shaft running speed is rather low in respect to the original spinning owing to Mach number preservation. Thus, the shaft stem has been selected accordingly. Refrigerant operational temperatures are strongly reduced in respect to a traditional turbocharger one. This is in favour of stability and safety. Sizes of the turbine inducer and exducer have been modified to meet the efficiency goal. Since the selected Expander Wheel and Shaft assembly establish the exit angle, it has been possible to calculate the exit pressure and triangles of velocity at any exducer diameter, taking the diffuser that is required to lower the axial velocity to about 10 m/s into consideration.

Since the flow angles at the rotor exit are known for any selected wheel, given the volumetric flow at the exducer exit, the tip diameter can be calculated. Inducer blade height is established by the flow angle at the rotor inlet and by the related volumetric flow.

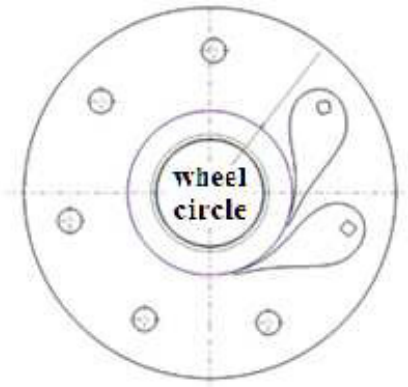

Fig. 8. Turbine nozzle vane arrangement

Nozzle vanes have been designed to reach the required velocity and

A- Center housing, rotating assembly and plate

B-Fluid conveyor and expander ssembly

Fig. 9. CEG details

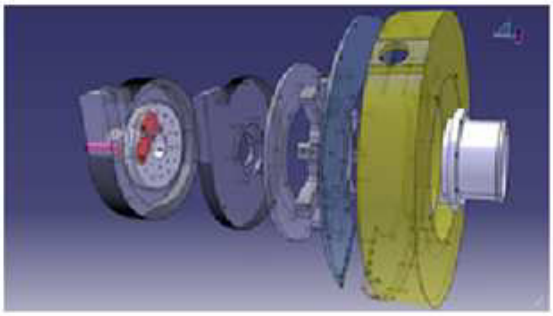

Fig.10. CEG exploded 3D representation

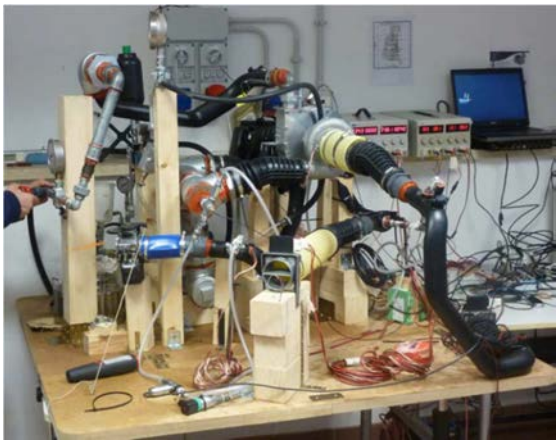

Fig.11. Compressed air operated test bench

the flow angle at the rotor inlet. Losses depend on the nozzle exit angle, on the channel length and passage size and shape. Nozzle blade trailing edge circle is suitably located upstream of the rotor leading edge circle. Fig. 8 shows the nozzle blades on the plate that contains the wheel. Moreover, a diffuser is located downstream of the exducer station to allow the best selection of the expander wheel exducer pressure that contributes to the wheel exit velocity triangle shape and size.

A ball bearing housing has been adopted mainly for two reasons: The first is related to the lower losses produced by the angular ball bearing cartridge and easy repair; the second is related to the lubrication aspects. The test bench is equipped with an oil lubrication system. The oil is the same used for main compressors of cryogenic plants. Theory and Tests made in the Roma Tre lab have shown that such an oil can safely be used to lubricate the bearing.

Fig. 9 shows details of the CEG assy and the expander inlet duct. Fig. 10 shows an exploded 3D drawing of the CEG components.

The CEG has been tested on a Roma Tre compressed air operated test bench (see Fig. 11). It has demonstrated the capability of continuous and safe running. Moreover, the air test results have been used to predict the CEG performance when the working fluid is a succedaneous one of the R404a. Such a forecast CEG performance has demonstrated that the built CEG would be capable to satisfy the needs for the R404a 100kW Cool Power Test bench.

5. Performance Tests and Results

The test bench for 100kW cool power has been equipped with the CEG. Fig. 5 shows the CEG installed inside the container that behaves as manifold for the RC and expander exit flows to be sent into the MC inlet. A photo of the whole bench is shown in Fig. 12. The test bench has been operated under Simple Cycle arrangement to evaluate the reference conditions.

At this research stage, the Test bench MC availability was for about 50kW cool power. Therefore, steady state conditions allowed the CEG to run under the derated behaviour at some 20 krpm. Thus, a sudden step opening of the condenser by-pass valve carried on full load CEG running tests.

Fig. 13 shows the pressure differences across the expander and the compressor versus the rotational speed. It can be seen that at the rotating velocity from 30 krpm to 40 krpm the pressure increase produced by the Recovery Compressor ranges from 80kPa to 100kPa. The expander pressure drop ranges from 4 to 5 bar when the rotational speed ranges from 35 to 40 krpm. Both these results are in the design expected values.

Fig. 12. The Test Bench

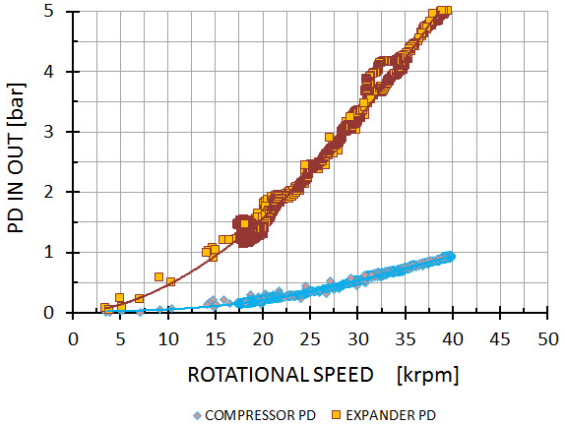

Fig. 13. Pressure difference versus rotational speed

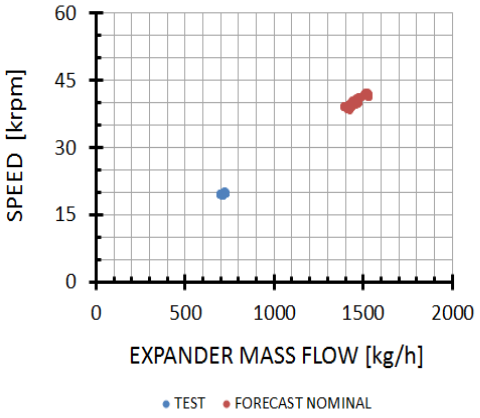

Fig. 14. Speed versus expander mass flow

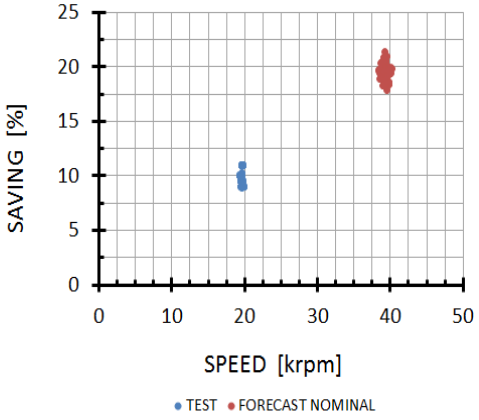

Fig. 15. Main Compressor Power saving versus rotational speed

Tests made keeping the condenser by - pass valve off, and operating the bleed valves to maintain the calculated superheating the test bench behaves under steady state conditions. The CEG velocity has been led at some 20 krpm producing a 20kPa pressure increase. The pressure drop across the expander has been some 150kPa. The test cool power was some 52 kW. Steady State speed versus expander mass flow is given in Fig.14, blue points represent the Steady State run at 20000 rpm with about 700 kg/h (194,4 g/s). Red points represent the predicted points corresponding to the blue ones, when the CEG machines would behave under similarity conditions at the nominal loading. Such values correspond to 100kW test bench cool power.

Main Compressor Power saving, in respect to that consumed in simple cycle arrangement is shown in Fig. 15. During the steady state behaviour of the test bench that makes the CEG run under derated conditions, the blue points can evidence some power saving of 10% 12%. In addition, in this case, the behaviour, for 100kW cool power has been simulated under similarity conditions. Some 18%-22% MCP saving has been predicted. The red point spot reports such a forecast. As soon as possible tests to validate the 100kW cool power test bench behaviour will be performed when the adequate MC will be available.

6. Conclusions

Cryogenic plant power consumption can be reduced by means of direct power regeneration. Internal cycles make the condensate subcool to increase before the main expansion valve and increase the pressure at the inlet of the Main Compressor. Saved power for optimum designed and matched systems is expected to be higher than 20%-22% in respect to that of the Simple Cycle.

The Compressor Expander Group behaviour, that increases the pressure at the Main Compressor inlet, has been demonstrated. The CEG can be obtained by modifying Car Engine Turbochargers, machining the compressor and expander wheels and remarking the casing. Nozzle has been designed for transonic flow expansion.

Tests have shown the feasibility of the concept and the saving that can be achieved.

Moreover, some evaluations on the possibility of using the liquid refrigerant R404a as lubricant for the ball bearing cartridge. The response is positive; tests will be done as possible. The adoption of hybrid bearings seems the most adequate for this application.

The bleed system for condensate subcooling including the CEG for Power Regeneration can be used to upgrade already existing plants. Some increase of the cool power, depending on the Refrigeration plant features, can be obtained, and a COP increase of some 22 – 23 %, is expected.

Acknowledgements

The Authors acknowledge the Italian Ministry for the Environment, Land and Sea; Angelantoni Industries S.p.A.; Se.Te.L S.r.l. and Roma Tre University for the COLD ENERGY Project Support.

References

[1] Borlein C. Energy Savings in Commercial Refrigeration Equipment: Low Pressure Control. White paper, Schneider Electric; August 2011.

[2] New Refrigeration Cycle to Improve 100 – Year - Old Technology. Calmac Manufacturing Corporation; October - December 2001.

[3] Minh NQ, Hewitt NJ, Eames PC. Improved Vapour Compression Refrigeration Cycles: Literature Review and Their Application to Heat Pumps. International Refrigeration and Air Conditioning Conference. Paper 795; 2006.

[4] Sarkar J. Ejector Enhanced Vapor Compression Refrigeration and Heat Pump Systems - A Review. Renewable and Sustainable Energy Reviews 16, 6647-6659; August 2012.

[5] Yu J, Zhao H, Li Y. Application of an Ejector in Auto Cascade Refrigeration Cycle for the Performance Improvement. International Journal of Refrigeration, vol.31, pp.279-286; 2008.

[6] Zhu Y, Jiang P. Hybrid Vapor Compression Refrigeration System with an Integrated Ejector Cooling Cycle. International Journal of Refrigeration, vol.35, pp. 68-78; 2012.

[7] Selvaraju A, Mani A. Experimental Investigation on R134a Vapor Ejector Refrigeration System. International Journal of Refrigeration, vol.29, pp.1160-1166; 2006.

[8] Kairouani L, Elakhdar M, Nehdi E, Bouaziz N. Use of Ejectors in a Multi- Evaporator Refrigeration System for Performance Enhancement. International Journal of Refrigeration, Vol.32, pp.1173-1185; 2009.

[9] Prakash A. Improving the Performance of Vapor Compression Refrigeration System by Using Sub – Cooling and Diffuser. International Journal of Engineering, Business and Enterprise Applications, ISSN (Print): 2279-0020, IJEBEA 13-129; 2013.

[10] Reddy KH *et al*. Improvement of Energy Efficiency Ratio of Refrigerant Compressor. International Journal of Scientific & Technology Research, Volume 2, ISSN 2277-8616, Issue 5; May 2013.

[11] Elgendy E. Parametric Study of a Vapor Compression Refrigeration Cycle Using a Two-Phase Constant Area Ejector. International Journal of Mechanical, Aerospace, Industrial and Mechatronics Engineering Vol.: 7 No: 8; 2013.

[12] Upadhyay N. To Study the Effect of Sub-Cooling and Diffuser on the Coefficient of Performance of Vapour Compression Refrigeration System. International Journal of Research in Aeronautical and Mechanical Engineering, Vol. 2, Issue. 6, pgs. 40-44; June 2014.

[13] Reindl DT, Hong H. Evaluation of Liquid Pressure Amplifier Technology, International Journal of Air Conditioning and Refrigeration, vol.13, pp.119-127; 2005.
[14] Hadawey A, Ge YT, Tassou S A. Energy Saving Trough Liquid Pressure Amplification in a Dairy Plant Refrigeration System. CEBER Brunel University Uxbridge Middlesex, UB8 3PH, UK.
[15] DOE, Liquid Refrigerant Pumping Technology for Improving Refrigeration Performance and Capacity, New Technology Demonstration Program, U.S. Department of Energy
[16] Taras MF, Lifson A, Dobmeier TJ. Refrigerant Cycle with Tandem Economized and Conventional Compressors. United States Patent; Patent No.: Us 6.955.058 B2; Date of Patent: Oct.18, 2005.
[17] Andres MJ. Expendable Turbine Driven Compression Cycle Cooling System. United States; Patent Application Publication; Pub. No.: Us 2007/0193301 A1; Pub. Date: Aug.23, 2007.
[18] Lifson A, Taras MF. Refrigerant System with Variable Capacity Expander. United States; Patent Application Publication; Pub. No.: Us 2010/0031677 A1; Pub. Date: Feb.11, 2010.
[19] Bush JW, Beagle WP, Mitra B. Refrigerating System with Parallel Staged Economizer Circuits Using Multistage Compression. United States; Patent Application Publication; Pub. No.: Us 2010/0223938 A1; Pub. Date: Sep.9, 2010.
[20] Mitra B, Beagle WP, Bush JW. Refrigerating System with Parallel Staged Economizer Circuits Discharging to Interstage Pressures of a Main Compressor. United States; Patent Application Publication; Pub. No.: Us 2010/0223939 A1; Pub. Date: Sep.9, 2010.
[21] Ascani M. Refrigerating Device and Method for Circulating a Refrigerating Fluid Associated With it. United States Patent; Patent No.: Us 8,505,317 B2; Date of Patent: Aug.13, 2013.
[22] Cerri G. A Simultaneous Solution Method Based on a Modular Approach for Power Plant Analyses and optimized Designs and Operations. International Gas Turbine and Aeroengine Congress and Exhibition, Birmingham, UK. ASME paper 96 –GT –302; June 10 – 13, 1996.
[23] Dixon SL, Hall CA. Fluid Mechanics and Thermodynamics of Turbomachinery. Butterworth Heinemann, Sixth Edition; 2010.
[24] Baljè OE. Turbomachines: A Guide to Design, Selection, and Theory. John Wiley and Sons, New York; 1980.
[25] Whitfield A, Baines NC. *Design of Radial Turbomachines*. John Wiley and Sons, New York, USA; 1990.
[26] Moustapha H *et al*. *Axial and Radial Turbines*. Edwards Brothers Incorporated, USA; 2003.
[27] Macchi E. Design Criteria for Turbines Operating with Fluids Having a Low Speed of Sound. Lecture Series 100, Von Karman Institute for Fluid Dynamics; 1977.
[28] Macchi E, Perdichizzi A. Efficiency Prediction of Axial-Flow Turbines Operating with Non-Conventional Fluids. ASME Journal of Engineering for Gas Turbines and Power; 1981, 103: 718-724.
[29] Cerri G. Organic Fluid Turbocharger for a 2000 kW Diesel Engine. International Gas Turbine Congress, Tokyo (Japan) 26 – 29 October 1987.
[30] Cerri G. Organic Fluid Turbines for Various Engine Power Level Turbochargers. 33rd ASME International Gas Turbine and Aeroengine Congress, Amsterdam (Netherlands); June 5 – 9, 1988, ASME pap. 88 – GT – 1.
[31] Cerri G. Turbosovralimentatori a Fluido Organico (ORC Turbochargers). Giornata di studio sulla sovralimentazione dei motori a combustione interna per autotrazione, Genoa; May 7, 1987.
[32] Wong CS, Meyer D, Krumdieck S. Selection and Conversion of Turbocharger as Turbo-Expander for Organic Rankine Cycle (Orc). 35th New Zealand Geothermal Workshop: 2013 Proceedings, Rotorua, New Zealand; November17 – 20, 2013.